Unconventional Quasiparticle Lifetime in Graphite

J. González,[1] F. Guinea,[2] and M. A. H. Vozmediano[3]
[1]*Instituto de Estructura de la Materia, Consejo Superior de Investigaciones Científicas, Serrano 123, 28006 Madrid, Spain*
[2]*Instituto de Ciencia de Materiales, Consejo Superior de Investigaciones Científicas, Cantoblanco 28049 Madrid, Spain*
[3]*Departamento de Matemáticas, Universidad Carlos III, Butarque 15, Leganés 28913 Madrid, Spain*
(Received 15 March 1996)

The influence of electron-electron scattering on quasiparticle lifetimes in graphite is calculated. In the limit when the Fermi surface is reduced to isolated points in the Brillouin zone, the suppression of screening leads to deviations from conventional Fermi liquid behavior. The inverse lifetime increases linearly with energy, in agreement with recent experiments. Similar features should also be present in narrow gap semiconductors and in carbon nanotubes. [S0031-9007(96)01496-2]

PACS numbers: 71.20.Tx, 73.50.Gr

Recent experiments [1] show that the inverse lifetime of quasiparticles in graphite increases linearly with energy over a broad energy range $\sim 0.3-4$ eV. The authors of Ref. [1] argue that this effect may be due to the unusual dispersion relation of plasmons in a 3D stack of conducting planes, where the electrons are confined to move in two dimensions [2]. In the present work, we analyze an alternative explanation of the energy dependence of the lifetime, although also associated to the electron-electron interaction. The main new feature in our model is the imperfect screening of the long range Coulomb interaction. In a conventional metal, the decay channels for quasiparticles are restricted, at low energies, by phase space limitations. A straightforward perturbative calculation, for short range interactions, gives that the inverse lifetime of a quasiparticle with energy ϵ above the Fermi level scales as ϵ^2. Hence, the width of the resonance associated to the quasiparticle is much less than its position. This fact justifies the use of an independent electron model for the low energy properties of metals.

Graphite is a semimetal. Band structure [3] calculations show that electrons are confined to narrow holes near the edges of the hexagonal Brillouin zone. The main features around the Fermi level are well described by a simple Hückel theory [4], which includes only the out of plane π orbitals located at each carbon atom. Intraplane hopping is much larger than the interplane hybridization. If we neglect the coupling between planes, the Fermi surface is reduced to two isolated points at the corners of the 2D Brillouin zone. The band dispersion is linear around these points, $\epsilon_k = \hbar v_{\mathrm{F}} |\vec{k}|$, where k is measured from the zone corners. In units of the hybridization between neighboring π orbitals, t, we find that $\hbar v_{\mathrm{F}} = 3ta/2$ where a is the distance between carbon atoms. The density of states is zero at the Fermi level, within this approximation. The long wavelength properties can be approximated by means of an effective 2D Dirac equation [5], instead of the more familiar effective mass approximation, used when the bands are parabolic at low energies.

Because of the vanishing density of states at the Fermi energy, the Coulomb interaction is not screened in a conventional fashion. Combining the band structure described above with the bare Coulomb interaction we obtain an effective Hamiltonian, for a single plane of graphite:

$$\mathcal{H} = \hbar v_{\mathrm{F}} \int d^2 r \bar{\Psi}(\vec{r}) \left(i\sigma_x \partial_x + i\sigma_y \partial_y \right) \Psi(\vec{r}) + \frac{e^2}{2\epsilon_0} \int d^2 r_1 \int d^2 r_2 \frac{\bar{\Psi}(\vec{r}_1)\Psi(\vec{r}_1)\bar{\Psi}(\vec{r}_2)\Psi(\vec{r}_2)}{|\vec{r}_1 - \vec{r}_2|} \tag{1}$$

where σ_x and σ_y are Pauli matrices, and Ψ is a two component spinor associated to the two bands which meet at the Fermi points. In a honeycomb carbon lattice, $t \approx 2.4$ eV. High energy screening processes are included in the effective dielectric constant, ϵ_0. We expect that (1) describes well the physics of a single layer of graphite for energies $\leq t$.

The Hamiltonian (1) defines a renormalizable theory [6] in the field theoretical sense [7–9]. Perturbation theory leads to logarithmic dependences on the high energy cutoff, which can be incorporated into new, renormalized, parameters in a standard way. The existence of logarithmic corrections can be inferred from the fact that the actual coupling constant in (1), $e^2/\epsilon_0 \hbar v_{\mathrm{F}}$, is dimensionless.

A detailed analysis of the renormalization procedure used to deal with the 2D Hamiltonian (1) is given in Ref. [6]. That scheme can be generalized to a system of weakly interacting planes. Interplane couplings can be of two types.

(i) Coulomb effects. They increase the number of diagrams that need to be calculated, as an electron in a given plane can be scattered by electron-hole pairs in other planes. The low energy properties are, however, not affected. The renormalization group (RG) scheme proceeds by integrating out slices in energy and momentum space. The momentum transfer in interplane processes is bounded by the inverse of the interlayer distance, d^{-1}. Thus, at sufficiently low scales, the electron-electron scattering retains the original dependence on the momentum transfer. The finite corrections induced by interplane Coulomb interactions can be included in a manner similar to the scheme used in Ref. [2]. The details are given below.

(ii) Interplane electron hopping. This interaction is responsible for the 3D features of the bands of graphite. It leads to deviations from the linear dispersion relation, used to define (1), at low energies. We expect that these deviations will become significant at energies comparable to the interplane hopping, ≈ 0.27 eV [3]. In addition, the density of states at the Fermi level becomes finite. Hence, metallic screening takes place at length scales greater than k_{FT}^{-1}, where $k_{\mathrm{FT}}^2 = 4\pi e^2 N(\epsilon_{\mathrm{F}})$. Because of the smallness of $N(\epsilon_{\mathrm{F}})$ [3], the associated energy scale, $\hbar v_{\mathrm{F}} k_{\mathrm{FT}}$ is much smaller than the previous one.

These effects are not included in the model described in (1). They influence the physics of the system at energies below their typical scales, mentioned above. Hence, the Hamiltonian (1) gives an effective description of graphite in an energy range bound by a lower cutoff ~ 0.2 eV, and a higher cutoff, where the bands can no longer be approximated by a linear dispersion relation, ~ 3–4 eV. This range comprises the experimental values analyzed in Ref. [1].

Quasiparticle lifetimes are also influenced by phonons [10], and by low energy, out of plane plasmons [11]. The phonon bandwidth in graphite is ~ 0.20 eV, and the out of plane plasmons have energies ~ 0.05 eV. Thus, for quasiparticle energies > 0.2 eV, these processes should give a constant contribution, independent of the quasiparticle energy.

A remarkable feature of the perturbation analysis of Hamiltonian (1) is that logarithmic divergences appear in the corrections to one particle properties, like the self energy, but electron-hole propagators are finite [6]. This reflects the fact that the divergences are due to the singularity of the interaction, and not to density of states effects. The intra Brillouin zone edge electron-hole propagator at low energies and momenta is [6]

$$\chi_0(\omega, \vec{q}) = \frac{\vec{q}^2}{32\pi\sqrt{v_{\mathrm{F}}^2 \vec{q}^2 - \omega^2}}, \qquad (2)$$

where χ_0 is purely real for $v_{\mathrm{F}}|\vec{q}| > \omega$, and purely imaginary otherwise. Thus, electron-hole pairs can be excited only if $v_{\mathrm{F}}|\vec{q}| < \omega$. This region is shown in Fig. 1.

The screened Coulomb potential, including interplane scattering, can be written as [2]

$$v_{\mathrm{scr}}(\omega, \vec{q}) = \frac{2\pi e^2}{\epsilon_0 |\vec{q}|} \times \frac{\sinh(|\vec{q}|d)}{\sqrt{[\cosh(|\vec{q}|d) + \frac{2\pi e^2}{\epsilon_0 |\vec{q}|} \sinh(|\vec{q}|d)\chi_0(\omega, \vec{q})]^2 - 1}}, \qquad (3)$$

where d is the distance between planes. It is interesting to note that Re v_{scr} has no poles at low energies, unlike the case of a stack of layers with quadratic dispersion, where a plasmon band, $\omega_p \propto |\vec{q}|$, was found [2]. We ascribe this difference to the fact that, in the present case, electron-hole pairs can exist only for $\omega > v_{\mathrm{F}}|\vec{q}|$, while in a conventional electron gas it is the opposite.

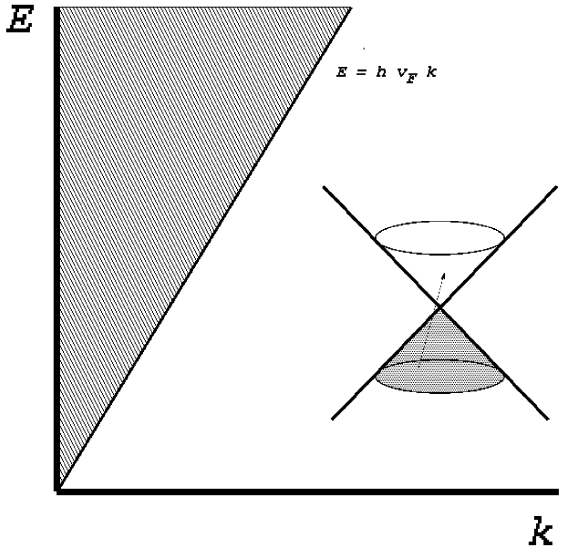

FIG. 1. Region in phase space available for electron-hole excitations. The nature of the interband *e*-*h* pairs is sketched in the diagram.

The quasiparticle lifetime can be obtained using standard RG methods. In the following, we study the lowest order diagram, neglecting the scaling of the Fermi velocity and wave function renormalization. The lowest order perturbative term is free of divergences (see below). Hence, following the preceding discussion, we do not expect qualitative changes when going to higher order. Using (3), the inverse of the quasiparticle lifetime can be written as

$$\mathrm{Im}\ \Sigma(\omega, \vec{k}) = \frac{2}{4\pi^2} \int d^2k' \frac{1 + \cos(\phi_{\vec{k}-\vec{k}'})}{2} \times \mathrm{Im}\ v_{\mathrm{scr}}(\omega - \epsilon_{k'}, \vec{k} - \vec{k}'), \qquad (4)$$

where $\phi_{\vec{k}-\vec{k}'}$ is the angle between vectors $\vec{k}$ and $\vec{k}'$, and we are summing over the two spins.

Expression (4) can be interpreted as the probability for a quasiparticle with frequency ω and momentum $\vec{k}$ to decay into a real quasiparticle of energy $\epsilon_{k'}$ and momentum $\vec{k}'$. Kinematical constraints in the phase space of final states imply that $\mathrm{Im}\ \Sigma(\omega, \vec{k}) \neq 0$ only if $\omega \leq v_{\mathrm{F}}|\vec{k}|$. This restriction seems incompatible with the phase space available for the creation of electron-hole pairs, shown in Fig. 1, suggesting that there are no channels for quasiparticle decay in the model described by (1).

We must, however, consider with care the limit $\lim_{\omega \to \epsilon_k + 0^+} \mathrm{Im}\ \Sigma(\omega, \vec{k})$. The simplest situation, which can be analyzed analytically, is the lowest order diagram shown in Fig. 2. For this case, $\mathrm{Im}\ \Sigma(\omega, \vec{k})$ drops discontinuously to zero at $\omega = v_{\mathrm{F}}|\vec{k}|$. The magnitude of the step is

$$\lim_{\omega \to \epsilon_k + 0^+} \mathrm{Im}\ \Sigma(\omega, \vec{k}) = \frac{1}{48} \left(\frac{e^2}{\epsilon_0 \hbar v_{\mathrm{F}}} \right)^2 \hbar v_{\mathrm{F}} |\vec{k}|. \qquad (5)$$

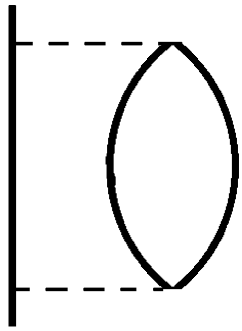

FIG. 2. Lowest order contribution to the quasiparticle lifetime.

The inverse lifetime, defined in this way, increases linearly with the energy of the quasiparticles. The real part of the self-energy shows a logarithmic dependence on the high energy cutoff needed to define the model (1), leading to non-Fermi liquid behavior [6]. The existence of a finite lifetime, despite the kinematical constraints described earlier, can be traced back to the divergence of the density of electron-hole pairs in the forward direction, $\omega = v_F|\vec{k}|$, which compensates exactly the reduction in the number of states in which the quasiparticle can decay as $\omega \to \epsilon_k$. Setting $\hbar v_F = 3/2ta$, where $t = 2.6$ eV, $a = 1.4$ Å, and $\epsilon_0 = 2.4$ [12], we find that the constant of proportionality between the inverse lifetime and the quasiparticle energy is 0.049 in $\mathrm{eV}^{-1}\,\mathrm{fs}^{-1}$. This value compares well to the experimental one, 0.029 $\mathrm{eV}^{-1}\,\mathrm{fs}^{-1}$ [1]. Note that the inverse lifetime should be an average of Im Σ over a finite interval of energies and momenta (see below), and expression (5) is an upper bound to such an average.

The behavior of Im $\Sigma(\omega, \vec{k})$ as $\omega \to \epsilon_k$, including the RPA and interplane interactions, can be calculated numerically, and it is shown in Fig. 3, using expression (4), with $d = 3.35$ Å and the parameters given above.

The kinematical constraints discussed earlier arise from the requirement of momentum conservation. In the presence of disorder, quasiparticles have a finite spread in momenta. Because of the sharp rise of Im Σ away from the line $\omega = \epsilon_k$, this spread leads also to a finite quasiparticle lifetime. This is shown in Fig. 4, where Im $\Sigma(\epsilon_k, |\vec{k}| - \Delta k)$ is plotted, with $\Delta k = 0.002$ $\mathrm{Å}^{-1}$. $(\Delta k)^{-1}$ corresponds, roughly, to the mean distance between scattering centers, in our case, $l \sim 500$ Å. Other inelastic scattering channels, such as phonons, will also contribute to give a spread in momentum and energy to the quasiparticles [10].

The lifetimes shown in Fig. 4 are consistent with the experimental observations [1]. The explanation that we propose here also implies non-Fermi liquid behavior in other properties of graphite, such as the conductivity or the susceptibility. Note, however, that we expect our model to break down at low energies, < 0.2 eV.

It was argued that low energy plasmons can be responsible for the unconventional quasiparticle lifetimes in graphite [1]. A layered 2D electron gas has plasmons above a certain threshold which depends linearly on momentum, $\omega_{pl} = v_{pl}|\vec{q}|$ [2]. These collective excitations give rise to a new decay channel for quasiparticles with velocity $v_{qp} = \hbar k/m > v_{pl}$. In most cases, decay into low energy plasmons cannot take place near the Fermi

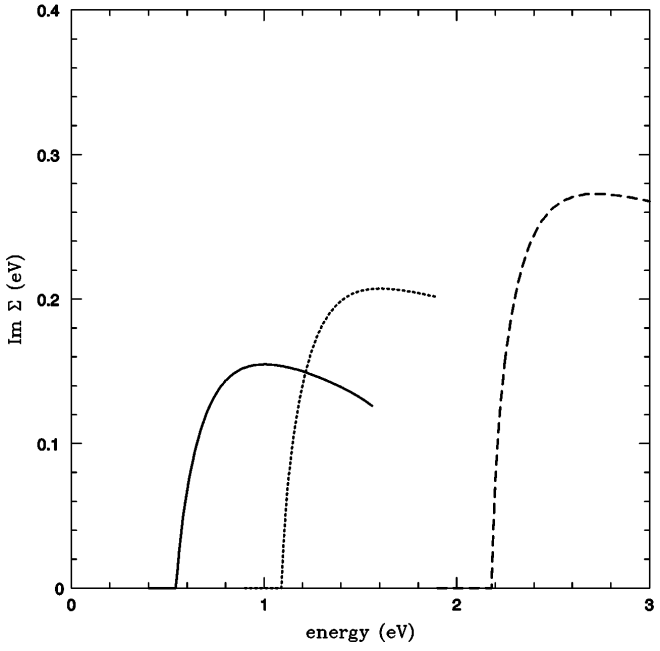

FIG. 3. Imaginary part of the self-energy as the function of frequency for various momenta: Solid line, $k = 0.1$ $\mathrm{Å}^{-1}$, dashed line, $k = 0.2$ $\mathrm{Å}^{-1}$, broken line, $k = 0.4$ $\mathrm{Å}^{-1}$.

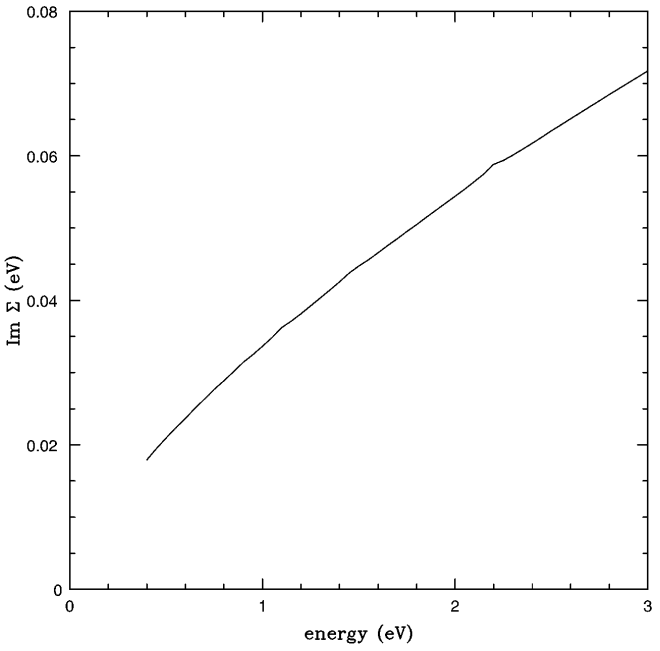

FIG. 4. Inverse quasiparticle lifetime, as defined in the text, as a function of the energy of the quasiparticle.

level, because $v_{\rm pl} > v_{\rm F}$. It is proposed in Ref. [1] that, in graphite, $v_{\rm pl} < v_{\rm F}$. The value of $v_{\rm F}/v_{\rm pl}$ scales as $[N(\epsilon_{\rm F})e^2 d]^{-1/2}$, where d is the interlayer distance and $N(\epsilon_{\rm F})$ is the density of states at the Fermi energy. Hence, the fact that $v_{\rm pl} < v_{\rm F}$ can be traced back to the low density of states at the Fermi level in graphite. Moreover, in a 2D free electron model, the density of states is independent of energy, so that the entire conduction band of graphite is assumed to have the same density of states. If we assume that the plasmon peaks lie within this *e-h* continuum, they will acquire a finite linewidth, which goes as the density of *e-h* pairs at low energies, $\propto \omega$. Thus, the plasmons cease to be well defined excitations, and the expressions from [2] should be replaced by more complex, nonanalytical, formulae. The model that we use, on the other hand, describes correctly the semimetallic character of graphite, and the increase in the density of states away from the Fermi level. Electron-hole excitations arise, mostly, from interband transitions. As we sum the RPA diagrams, plasmonlike excitations are included in (3). Thus, we think that our model provides a more adequate description of decay processes in graphite.

The results depicted in Fig. 4 have been obtained by combining a many loop propagator, the RPA bubble modified by interplane effects, with a zero loop description of the quasiparticles. We neglect the renormalization of the quasiparticle pole, calculated in [6]. As we scale towards low energies, the quasiparticle pole loses spectral strength, in the manner analyzed in [6]. We expect, however, the main result of this Letter, shown in Fig. 4, to be weakly dependent on this renormalization. Unlike in 1D conductors, the Hamiltonian (1) flows towards a free fixed point [6], which makes plausible the use of unrenormalized quasiparticle propagators in the calculation of the lifetimes. Note, however, that the bare coupling constant, $e^2/\epsilon_0 \hbar v_{\rm F}$, is of order unity, although most likely reduced by density of states factors, $\sim (2\pi)^{-2}$.

The main physical basis for the unconventional dependence of the quasiparticle lifetimes in energy, and the deviation from Fermi liquid theory, lies in the absence of metallic screening. As mentioned before, this picture does not hold for energies sufficiently close to the Fermi energy, $\epsilon - \epsilon_{\rm F} \sim 0.2$ eV, where we expect conventional Fermi liquid behavior to be restored. Note, however, that the model in (1) describes correctly the low energy physics of a single graphite sheet, or single sheet carbon nanotubes [14].

We expect that other semimetals may exhibit similar behavior. In particular, it is well known that the band structure of zero gap semiconductors can be approximated by the 3D Dirac equation [13]. In these materials, a description similar to the one used here should be valid down to the lowest energies. Hence, the model in (1), and extensions of it, are capable of describing realistic systems which deviate from non-Fermi liquid behavior beyond one dimension.

Note added.—After this manuscript was submitted for publication, a comment and a reply on the experiments reported in [1] were published [15]. We agree with the main issue raised in the Comment (a layered Fermi liquid shows a conventional quasiparticle lifetime). The reply affirms that the band structure in graphite differs significantly from that of a Fermi liquid, and suggests an alternative dispersion relation. We agree with the first statement, but we find that a more realistic band structure is the one used in this Letter.

[1] S. Yu, J. Cao, C. C. Miller, D. A. Mantell, R. J. D. Miller, and Y. Gao, Phys. Rev. Lett. **76**, 483 (1996).

[2] P. Hawrylak, G. Eliasson, and J. J. Quinn, Phys. Rev. B **37**, 10 187 (1988).

[3] A. Zunger, Phys. Rev. B **17**, 626 (1978).

[4] E. Hückel, Z. Phys. **83**, 632 (1933).

[5] J. González, F. Guinea, and M. A. H. Vozmediano, Phys. Rev. Lett. **69**, 172 (1992); J. González, F. Guinea, and M. A. H. Vozmediano, Nucl. Phys. **B406**, 771 (1993).

[6] J. González, F. Guinea, and M. A. H. Vozmediano, Mod. Phys. Lett. B **7**, 1593 (1994); Nucl. Phys. **B424**, 595 (1994); J. Low. Temp. Phys. **99**, 287 (1995).

[7] R. Shankar, Rev. Mod. Phys. **66**, 129 (1994).

[8] J. Polchinski, in *Proceedings of the 1992 TASI in Elementary Particle Physics*, edited by J. Harvey and J. Polchinski (World Scientific, Singapore, 1992).

[9] J. González, M. A. Martín-Delgado, G. Sierra, and M. A. H. Vozmediano, *Quantum Electron Liquids and High-T_c Superconductivity* (Springer-Verlag, Berlin, 1995).

[10] F. Guinea, J. Phys. C **14**, 3345 (1981).

[11] R. C. Tatar and S. Rabii, Phys. Rev. B **25**, 4126 (1982); E. J. Jensen, R. E. Palmer, W. Allison, and J. F. Annett, Phys. Rev. Lett. **66**, 492 (1991); P. Leitenberger and R. E. Palmer, Phys. Rev. Lett. **76**, 1952 (1996).

[12] E. A. Taft and H. R. Phillipp, Phys. Rev. **138**, A197 (1965).

[13] See, for instance, M. Balkanski, in *Elementary Excitations in Solids, Molecules and Atoms*, edited by J. T. Devreese, A. B. Kunz, and T. C. Collins (Plenum, New York, 1974).

[14] S. Ijima, Nature (London) **354**, 56 (1991).

[15] L. Zheng and S. Das Sarma, Phys. Rev. Lett. **77**, 1410 (1996); S. Yu, J. Cao, C. C. Miller, D. A. Mantell, R. J. D. Miller, and Y. Gao, *ibid.* **77**, 1411 (1996).